Systematics, Morphology and Biogeography

Phyllocnistis hemera sp. nov. (Lepidoptera: Gracillariidae): a new species of leaf-miner associated with *Daphnopsis fasciculata* (Thymelaeaceae) in the Atlantic Forest

Júlia Fochezato[a], Rosângela Brito[a], Rosy Mary dos Santos Isaias[b], Gislene Lopes Gonçalves[c,d], Gilson R.P. Moreira[a,*]

[a] Universidade Federal do Rio Grande do Sul, Instituto de Biociências, Departamento de Zoologia, Porto Alegre, RS, Brazil
[b] Universidade Federal de Minas Gerais, Instituto de Ciências Biológicas, Departamento de Botânica, Belo Horizonte, MG, Brazil
[c] Universidade Federal do Rio Grande do Sul, Instituto de Biociências, Departamento de Genética, Porto Alegre, RS, Brazil
[d] Universidad de Tarapacá, Facultad de Ciencias Agronómicas, Departamento de Recursos Ambientales, Arica, Chile

ARTICLE INFO

ABSTRACT

During recent studies performed in the Atlantic Forest, a new species of Phyllocnistinae (Gracillariidae), *Phyllocnistis hemera* **sp. nov.**, leaf miner of *Daphnopsis fasciculata* (Thymelaeaceae) was discovered. The adults are described and illustrated as well as the immature stages, with notes on natural history including a description of the leaf mine. Additionally, DNA barcode sequences were compared to other representatives of Phyllocnistinae to test for the specific status of *P. hemera* and to infer phylogenetic relationships. This is the fifth species described for the genus *Phyllocnistis* in the Atlantic Forest and the first record of a gracillarid mining Thymelaeaceae leaves.

© 2017 Sociedade Brasileira de Entomologia. Published by Elsevier Editora Ltda. This is an open access article under the CC BY-NC-ND license (http://creativecommons.org/licenses/by-nc-nd/4.0/).

Introduction

The Gracillariidae (Lepidoptera) is one of the most diverse families of leaf mining microlepidoptera. Approximately 2000 species have been described in 106 genera, with cosmopolitan distribution but not found in the Antarctic region (Davis, 1987; De Prins and De Prins, 2017). Kawahara et al. (2017) carried out a phylogenetic analysis and proposed a new classification for the group, dividing Gracillariidae into eight subfamilies. The Phyllocnistinae, one of the subfamilies retained in the new classification, has been the recent focus of taxonomic studies of the Neotropical region (Kawahara et al., 2009; Davis and Wagner, 2011; Brito et al., 2012; De Prins et al., 2016; Brito et al., 2017a,b).

Phyllocnistinae is a monotypic subfamily represented by species of *Phyllocnistis* Zeller, 1848. This genus has currently 108 species described worldwide, but only 27 for the Neotropics (De Prins and De Prins, 2017; Brito et al., 2017a). Representatives of this genus can be distinguished from the other gracillariids by a set of typical fasciae and strigulae on the forewings, and by a set of tergal spines on the abdominal segments on the pupae. The larvae usually present three sap-feeding instars followed by a spinning instar (Davis, 1987). The sap-feeding instar feeds on cell fluid which is released by the laceration of leaf tissue; the spinning instar, which does not feed, is responsible for the construction of a silk cocoon within which pupation occurs. Only two species, *P. citrella* Stainton and *P. tethys* Moreira & Vargas, have information regarding the type of tissue used as food by the sap-feeding larvae. Those of *P. citrella* are known to feed on epidermal cells, while larvae of *P. tethys* feed upon the spongy tissue (Achor et al., 1997; Brito et al., 2012).

Hostplants are known only for a third of the species of *Phyllocnistis*. They belong to 34 families of angiosperms, 13 of which occur in the Neotropics (De Prins and De Prins, 2017). Recently, during collections performed in the Atlantic Forest, in southern Brazil, a gracillariid representative associated with Thymelaeaceae was found for the first time. The comparison at both morphological and molecular levels confirmed that it is a new *Phyllocnistis* species. Here we provide illustrations and description of the corresponding adult and immature stages, and highlight important characteristics regarding its life history and feeding habits in association with the characterization of the leaf mine. DNA barcode (COI) was obtained from some specimens in order to establish the specific status and its phylogenetic relationships with representatives of the Phyllocnistinae.

Material and methods

The specimens were reared in small plastic vials under controlled abiotic conditions (14 h light/10 h dark; 25 ± 2 °C) at the *Laboratório de Morfologia e Comportamento de Insetos, Departamento de Zoologia, Universidade Federal do Rio Grande do Sul* (UFRGS), Porto Alegre, Rio Grande do Sul state (RS), Brazil, during May 2016, January, June and July 2017. They came from field-collected leaf mines associated with the host plant *Daphnopsis fasciculata* (Meisn.) Neveling (Thymelaeaceae), at the *Centro de Pesquisa e Conservação da Natureza* (CPCN Pró-Mata/PUCRS 29°28′36″ S, 50°10′01″ W), São Francisco de Paula, RS.

Morphological analysis

Adults were pinned and dried. Immature stages were fixed with Dietrich's fluid and preserved in 75% ethanol. At least 3 specimens of each stage were used to describe the immatures. For adult gross morphology the specimens were cleared in 10% potassium hydroxide (KOH) and slide-mounted in Canada balsam. Morphological analysis and descriptions were performed with the aid of a Leica® M125 stereomicroscope with an attached Sony® Cyber-shot DSC-H10 digital camera for photography. Genitalia structures were analyzed and photographed with a Nikon AZ 100 M stereomicroscope. The software CorelDraw® X8 and Corel Photo Paint® X8 were used for vectorization and image processing. The terminology used for the description of forewing pattern and genitalia follows Brito et al. (2017b) and Kobayashi and Hirowatari (2011), respectively.

For scanning electron microscopy, specimens were dehydrated in a Bal-tec® CPD030 critical-point drier, mounted on metal stubs with double-sided tape and coated with gold in a Bal-tec® SCD050 coater. Photographs were taken under a JEOL® JSM5800 scanning electron microscope at the *Centro de Microscopia Eletrônica* (CME), UFRGS.

For histological sections, leaf fragments (0.5 cm^2) with mines ($n = 6$) were fixed in FAA (37% formaldehyde, acetic acid, 50% ethanol, 1:1:18, v/v) for 48 h, dehydrated in an n-butyl series, embedded in Paraplast and sectioned transversely (12 μm) in a rotary microtome (Jung Biocut). The sections were stained in safranin-astrablue (2:8, v/v) (Bukatsch, 1972, modified to 0.5%), and mounted in colorless varnish (Paiva et al., 2006). Photographs were taken under a Leica DM 2500-LED light microscope with a Leica DFC 7000T camera.

Museum collections

The material examined was deposited in the following entomological collections:

LMCI Laboratório de Morfologia e Comportamento de Insetos, Universidade Federal do Rio Grande do Sul, Porto Alegre, Brazil
MCTP Museu de Ciências e Tecnologia da Pontifícia Universidade Católica do Rio Grande do Sul, Porto Alegre, Brazil

Molecular analysis

Genomic DNA was extracted from larval tissue of three specimens of *P. hemera* (LMCI 292-25C, D and E) using the Purelink genomic DNA extraction kit (Invitrogen) following manufacturer's instructions. Polymerase chain reaction (PCR) was performed to amplify the DNA barcode region (sensu Hebert et al., 2003), i.e. a 660-base pair (bp) segment of the mitochondrial gene cytochrome c oxidase subunit I (CoI), with the universal primers and conditions proposed by Folmer et al. (1994). Variants obtained matched the region sequenced in other *Phyllocnistis* deposited in the GenBank and BOLD Systems databases. PCR products were treated

Table 1

Specimens used in this study to infer the specific status of *Phyllocnistis hemera* and phylogenetic relationship within the genus.

Group	Genus	Species	Acession number	
			Genbank	BOLD systems
Ingroup	*Phyllocnistis*			
		citrella	KF919121	GREC094-12
		gracilistylella	AB614510	–
		hemera sp.n.	MG264519	MISA019-17
		hyperpersea	HQ971045	RDOPO395-10
		magnoliella	KF492018	LTOL1038-11
		ourea	KY006927	MISA013-16
		saligna	AY521491	–
		selene	KY006929	MISA015-16
		phoebus	KY006928	MISA014-16
		perseafolia	HM382097	RDOPO394-10
		populiella	KR941466	CNRVE3067-15
		tethys	JX272049	–
		vitegenella	KR938941	–
Outgroup	*Angelabella*			
		tecomae	KM983605	–
	Marmara			
		arbutiella	FJ412783	LBCS922-07

with exonuclease I and FastAP thermosensitive alkaline phosphatase (Thermo Scientific), sequenced using BigDye chemistry and analyzed in an ABI3730XL (Applied Biosystems). Sequences were automatically aligned using the algorithm Clustal X in MEGA v5 (Tamura et al., 2011) running in full mode. Data generated in this study were deposited in GenBank and BOLD (Table 1).

Phylogenetic trees were reconstructed to test the specific status of the new species and to infer its relationships within the genus. Representative taxa belonging to *Phyllocnistis* were incorporated, particularly Neotropical species already described (Table 1). The tree was rooted with species of *Angelabella* Vargas & Parra and *Marmara* Clemens and representatives of the subfamilies Oecophyllembiinae and Marmarinae, known to be closely related to Phyllocnistiane (Kawahara et al., 2017).

Phylogenetic reconstruction used distance (neighbor-joining [NJ]) and model-based methods (Maximum Likelihood [ML] and Bayesian Inference [BI]). The substitution model GTR+G was used for ML and BI according to the Akaike Information Criterion (AIC) performed in MEGA v5. The NJ and ML analyses were run in MEGA v5 using default parameters for tree inference. Monophyly confidence limits were assessed with the bootstrap method (Felsenstein, 1985) at 60% cutoff after 1000 bootstrap iterations. The BI analysis was implemented in BEAST v1.8.4 (Drummond et al., 2012), using an uncorrelated lognormal clock and a Yule prior on branching rates. Four independent runs of 10 million generations and a burn-in period of 10,000 (the first 1000 trees were discarded) were implemented; the remaining trees were summarized in TreeAnnotator v1.6.2 (Drummond and Rambaut, 2007) and used to infer a maximum a posteriori consensus tree. Bayesian posterior probabilities (BPP) were used as an estimate of branch support. Consensus trees were visualized and edited in FigTree 1.4.2 (http://tree.bio.ed.ac.uk/software/201/). The genetic distances between the same pairs of taxa used in the phylogenetic analysis (including outgroups) were analyzed using the Kimura 2-parameter (K2P) model, with 1000 bootstrap replications in MEGA v5.

Results

Phyllocnistis hemera Brito & Fochezato **sp. nov.** (Figs. 1–7)

Type material. MALE HOLOTYPE: São Francisco de Paula municipality, Rio Grande do Sul (RS), Brazil; preserved pinned and dried,

reared from a mine associated with *D. fasciculata*, 22–24.VI.2016, G.R.P. Moreira, R. Brito and J. Fochezato colls. (LMCI306-47). PARATYPES: Same locality, 28-30.VI.2017, G.R.P. Moreira and J. Fochezato coll., two males (LMCI 319-30 and 319-36) and two females (LMCI 319-35 and 319-45); 22–24.VI.2016, G.R.P. Moreira, R. Brito and J. Fochezato coll., one male (LMCI 306-46) and one female (LMCI 306-43) donated to MCTP (60251, 60252, respectively); 01–02.VII.2017, G.R.P. Moreira and J. Fochezato coll., one female (LMCI 320-43), donated to MCTP (60253).

Additional specimens examined from the same locality and host plant, all preserved pinned and dried: 22–24.VI.2016, G.R.P. Moreira, R. Brito and J. Fochezato colls., four males (LMCI 306-26, 32, 36 and 40) with genitalia on slides (GRPM 50-144 to 147, respectively); three females (LMCI 306-34, 35 and 49) with genitalia on slides (GRPM 50-148 to 150, respectively); 28–30.VI.2017, G.R.P. Moreira and J. Fochezato colls., one male (LMCI 319-69).

Additional immature specimens of *P. hemera* were deposited at LMCI, all dissected from leaf mines of *D. fasciculata* collected at the type locality: 10–13.II.2015, G.R.P. Moreira and R. Brito coll., preserved in 100% ethanol at −10 °C and used for DNA extraction (LMCI 292-25); 28–30.VI.2017, G.R.P. Moreira and J. Fochezato coll. and preserved in 75% ethanol. Eight sap-feeding larvae (LMCI 319-9), three spinning larvae (LMCI 319-8) and three pupae (LMCI 319-7) were used for microscopic studies. Additionally, nine leaf mine fragments containing sections of *P. hemera* mines (LMCI 320-9 to 11) from the type locality were fixed and preserved in FAA as described above, and used in the histological sections, 01–02.VII.2017, G.R.P. Moreira and J. Fochezato coll.

Diagnosis. *P. hemera* adults are easily distinguished from the other Neotropical *Phyllocnistis* by a longitudinal fascia on the forewing with superior border enlarged, reaching the costal margin. Its pupal stage is similar to that of *P. drimiphaga* Kawahara, Nishida & Davis in having the cocoon-cutter divided into three processes, the central longer than the lateral ones, and by the similar arrangement of tergal spines on abdominal segments. However, *P. hemera* has lateral processes shorter and wider than *P. drimiphaga*, and two pairs of setae on the clypeus, while *P. drimiphaga* has only one pair. The spinning larva of *P. hemera* is similar to that of *P. ourea* Brito & Moreira, as both share ventral ambulatory, single callus on central meso- and metathorax. However, these species differ in the location of the ventral calli on the abdominal segments (Ab); *P. hemera* has ventral calli on abdominal segments 3 to 7 (Ab 3–7), while *P. ourea* has calli on Ab 3–6.

Description. *Adult* (Fig. 1). Male and female similar in size and color. Forewing length 3.51–4.17 mm ($n = 5$). Head: antennae silver, ~ the length of forewing. A pair of tufts formed by a set of scales emerging from the base of antenna are directed to the frons.

Labial palp slender, silver, ~0.5 mm in length. Proboscis without scales. Thorax: Forewing ground color white silver, with light yellow fasciae bearing brown borders. Longitudinal fascia with well-marked border, which is much wider and convex on the basal half, reaching the costal margin; longitudinal fascia emerges from the wing base toward the median region, being completely connected to the first transverse fascia. The latter emerges on the costal margin and is slightly connected to the second transverse fascia. The second transverse fascia crosses the wing from the costal margin toward the inner margin; it is disconnected from the third and fourth fascia. Last two fasciae fused, forming a blotch on the distal region. Costal strigulae emerge from second, third and fourth transverse fasciae. Apical strigulae emerge from apical spot. Inner marginal fringes mostly light brown. Abdomen: covered with silver scales.

Male genitalia (Fig. 2A–D). One pair of coremata located between the intersegmentary membrane of Ab 8 and 9; the coremata are formed by a set of long, fine scales, reaching ~0.4× the size of valvae (Fig. 2B and C). Uncus absent. Tegumen narrow at base, widening toward the apex, forming a dorsal sclerotized arch; small setae occur next to the lateral borders of the tegumen; tuba analis narrow and membranous, surpassing the distal margin of tegumen. Valvae digitiform, slightly narrower and finer on base, widening toward the apex. Setae vary in size from small to medium on ventral distal region, forming a line; along the valva, setae varying in size are randomly arranged (Fig. 2A and C). Saccus U-shaped. Phallus elongated, weakly sclerotized, cylindrical and partially wrinkled, with fine apex. Cornuti absent (Fig. 2D).

Female genitalia (Fig. 2E–G). Anterior and posterior apophyses similar in shape; the posterior half the size of the anterior; the posterior apophyses reach Ab 8 and the anterior ones the posterior portion of Ab 7. Anal papillae with medium-sized setae, randomly arranged. Ostium bursae located on median region of the eighth abdominal sternum; ductus bursae long, membranous and slender; corpus bursae ellipsoid and membranous; signum wide, slightly rectangular with two spines on the proximal margin; one acute, well developed, the other of reduced size (Fig. 2E–G). Variation in these structures was found, such as: (1) one of the signa with an acute spine, the other without spines; (2) both signa bearing well developed spines; (3) one single signum containing a spine with bifurcated apex.

Immature stages

Sap-feeding larva (Figs. 3A, 4 and 7D). Leaf miner, flattened dorsoventrally (Fig. 4D), hypermetamorphic, presenting three instars. Body light yellow, 5.39–7.67 mm (min–max length); average last instar head capsule width ~0.64 mm ($n = 5$) (Fig. 7D). Head: prognathous, setae absent; labrum slightly bilobed with small hypopharyngeal spines next to lateral margin. Labium shaped like the labrum, however wider and with greater number of spines

Fig. 1. Adult of *Phyllocnistis hemera*, dorsal view: (A) wings spread, pinned and dried (LMCI 306-47); (B) wings folded, on *Daphnopsis fasciculata* leaf surface. Scale bars: 1 mm.
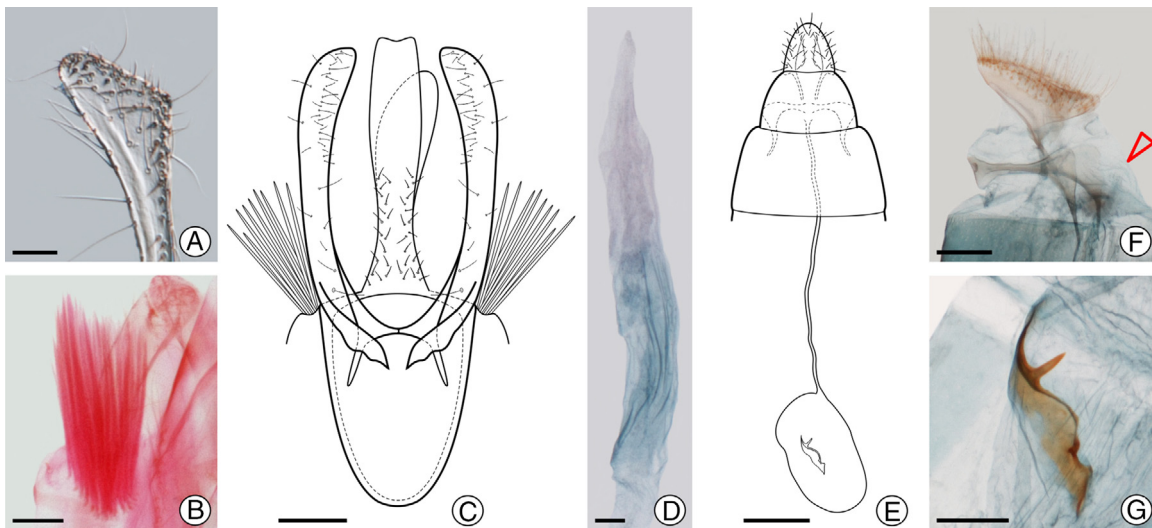
Fig. 2. *P. hemera* genitalia under light microscopy: (A–D) male genitalia; (E–G) female genitalia. (A) apex of left valva, mesal view (LMCI 319-69); (B) left corema, ventral (LMCI 306-26); (C) male genitalia, ventral; (D) aedeagus, lateral (LMCI 306-36); (E) female genitalia, ventral; (F) female last abdominal segments, lateral (LMCI 306-49) with the ostium bursae indicated by arrow; (G) signum in detail, ventral (LMCI 306-49). Scale bars: 50 (A, B, D), 100 (C, F, G), 400 μm (E).
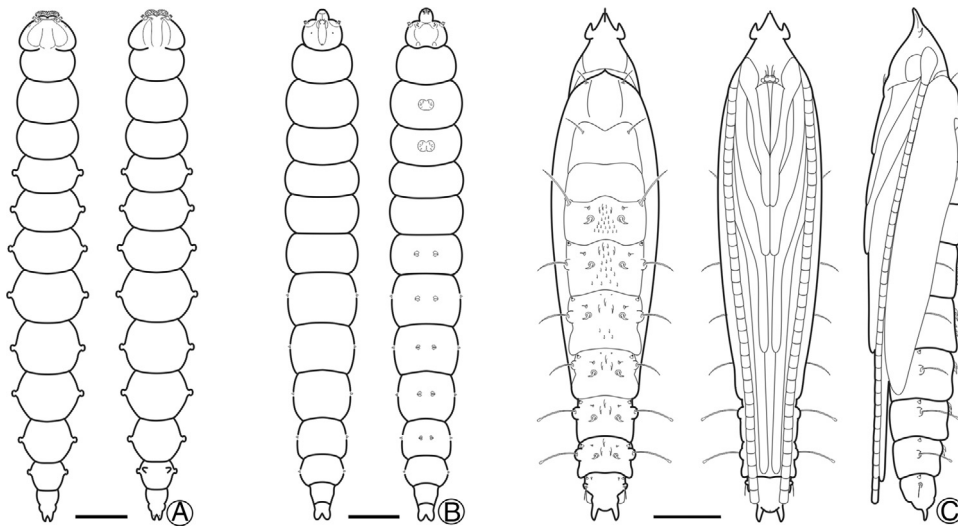

Fig. 3. Larval and pupal morphology of *P. hemera* under light microscopy: (A) sap-feeding larva, dorsal and ventral views; (B) spinning larva, dorsal and ventral; (C) pupa, dorsal, ventral and lateral, respectively. Scale bars: 500 μm.

(Fig. 4A–C and E); a small aperture on labium indicating the rudimentary spinneret (Fig. 4F). Labial and maxillary palpi absent. Antenna 3-segmented; the second segment with two sensilla, the distal one with a single apical sensillum (Fig. 4G). On anterior section of lateral region of the head, one rounded stemma followed by a microseta (Fig. 4H). Thorax: without setae, legs absent; presence of one pair of latero-dorsal prothoracic spiracles, with peritreme not differentiated (Fig. 4I). Abdomen: setae, prolegs and calli absent; a pair of laterodorsal lobes from first to eighth abdominal segment (Fig. 4J and M–N). These lobes are dorsoventrally flattened; on Ab 8 there is a second pair of lateroventral lobes with fine apex (Fig. 4K and L); last abdominal segment slightly divided, with pairs of microsetae on ventral region (Fig. 4O).

Spinning larva (Figs. 3B, 5 and 7E). Endophyllous, cylindrical, with coloration similar to the sap-feeding larva, 5.47–6.04 mm (min–max length). Body covered with microtrichia. Head: setae absent or reduced, except for three pairs located on the clypeal region; buccal apparatus modified into an anteriorly located, trophic lobe presenting corrugated tegument (Fig. 5A, B, D and E). Labial palpi absent; maxilla represented by three pairs of small setae. The trophic lobe in ventral view is long, with functional apical aperture (Fig. 5C). Antennae short, 3-segmented; three sensilla emerge from the second segment and one, bristle-like seta from the apical segment (Fig. 5H). Thorax: setae reduced or absent. Legs absent; prothoracic shield slightly evident, represented by an irregular, corrugated, central area (Fig. 5F). Laterally on prothoracic tergum one pair of rounded spiracles, with peritreme slightly elevated (Fig. 5G). A single ambulatory callus centrally on ventral region of meso- and metathorax; slightly divided on metathorax (Figs. 3B and 5I and J). Abdomen: one pair of ambulatory calli ventrally on Ab 3–7 (Figs. 3B and 5M and N), smaller compared to those on meso- and metathorax. One pair of small lateral sensilla on Ab 4–7 (Fig. 5L), which decrease in size antero-posteriorly. Last abdominal segment partially divided into two lobes (Fig. 5K) with two pairs of microsetae on ventral region (Fig. 5O).

Pupa (Figs. 3C, 6 and 7G). Dark brown (Fig. 7G), 3.92–4.08 mm (min–max length). Cocoon-cutter with three projections; the central one lanceolate, longer and wider, with serrated border; the lateral ones shorter, hook-shaped (Fig. 6A–B and D). Clypeus slightly bilobed, with two pairs of small setae (Fig. 6B). Antenna long
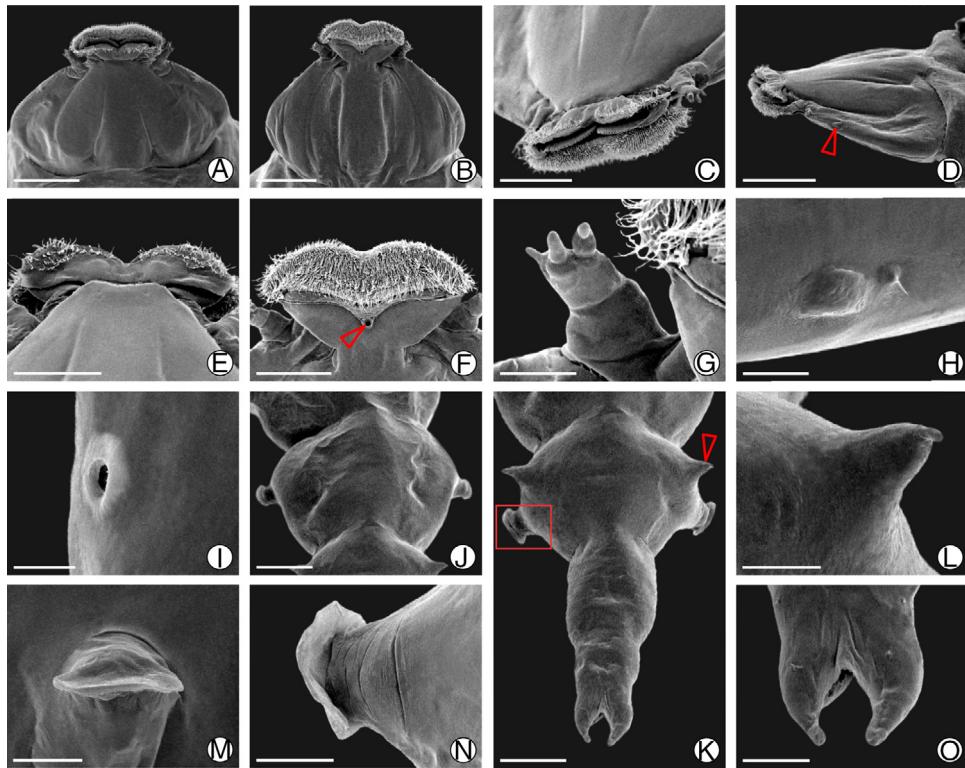
Fig. 4. Scanning electron micrographs of *P. hemera* sap-feeding larva: (A–D) head under dorsal, ventral, anterior and lateral views (arrow indicates stemma); (E) labrum, dorsal; (F) labium, ventral (arrow indicates spinneret aperture); (G) antenna, ventral; (H) stemma in detail (indicated by arrow in D), lateral; (I) prothoracic spiracle, dorsal; (J) segment A7, ventral; (K) segments A8-10, ventral; (L) detail of latero-ventral lobe indicated by arrow in K, ventral; (M, N) latero-dorsal lobe, highlighted by the red rectangle in K, lateral and dorsal; (O) last abdominal segment, ventral. Scale bars: 200 (A, B, D, K), 70 (C), 100 (E, F, O), 30 (G), 20 (H), 10 (I), 250 (J), 25 (L), 50 (M), 40 μm (N).
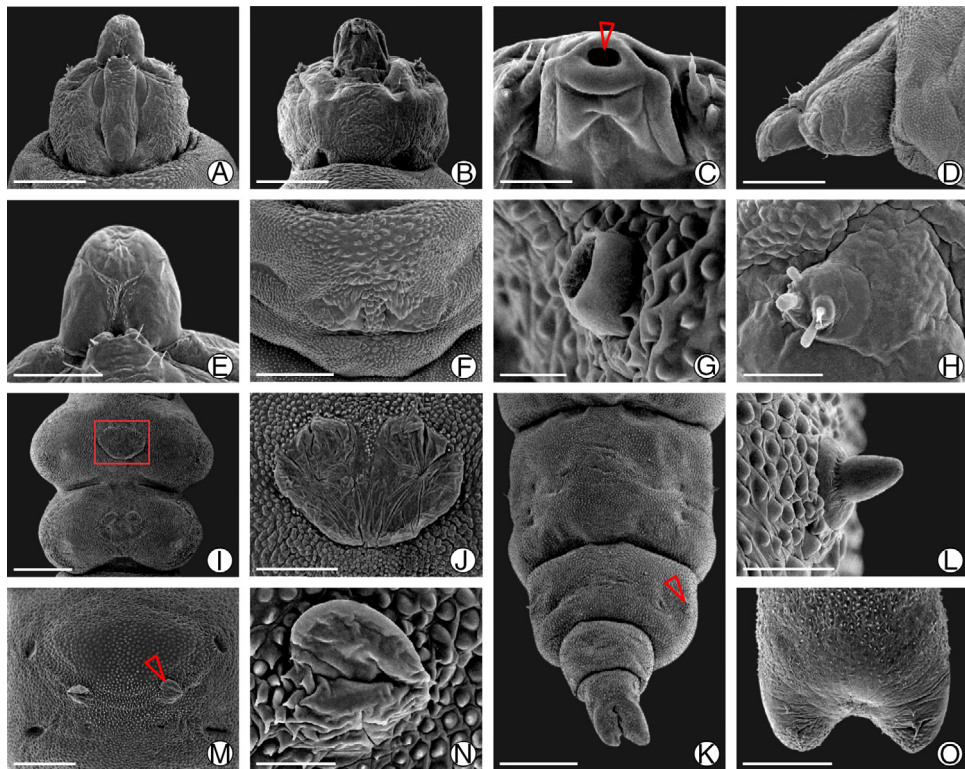
Fig. 5. Scanning electron micrographs of *P. hemera* spinning larva: (A, B) head, dorsal and ventral views; (C) spinneret, antero-lateral (arrow indicates functional aperture); (D) head, lateral; (E) detail of trophic lobe, dorsal; (F) prothoracic shield, dorsal; (G) prothoracic spiracle, lateral; (H) antenna, anterior; (I) meso- and metathoracic calli, ventral; (J) mesothoracic callus in detail (indicated by rectangle in I), ventral; (K) abdominal segments Ab 7-10, dorsal; (L) latero-sensillum indicated by arrow in K, dorsal; (M) abdominal segment Ab 7, ventral (arrow indicates one of the calli); (N) callus in detail, ventral (indicated by arrow in M); (O) last abdominal segment, ventral. Scale bars: 200 (A, B, D, E, K), 150 (C,F), 10 (G, N), 20 (H, L), 250 (I), 80 (J, O), 100 μm (M).
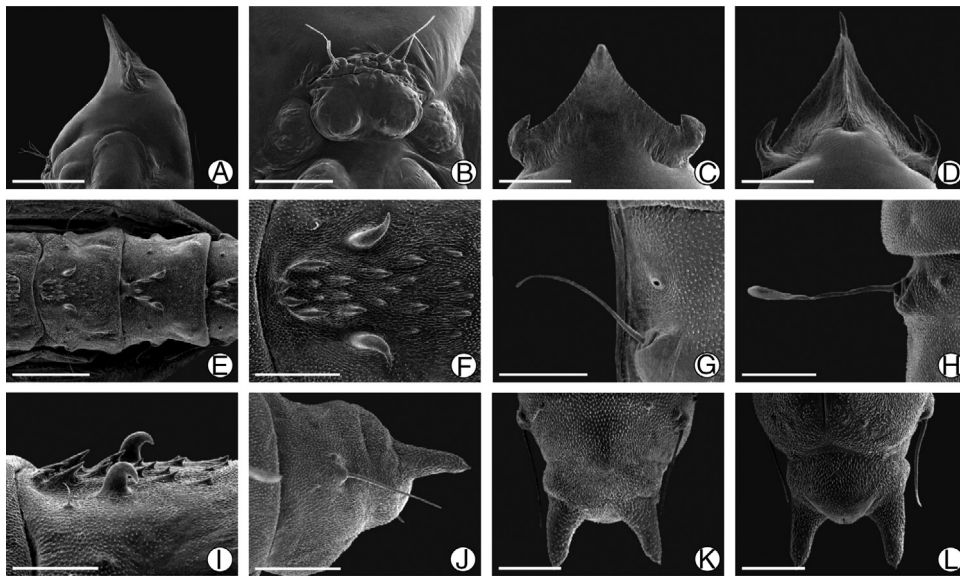
Fig. 6. Scanning electron micrographs of *P. hemera* pupa: (A) head, lateral view; (B) setae over clypeus, ventral; (C, D) cocoon-cutter, ventral and dorsal; (E) terga of abdominal segments Ab 3-4, dorsal; (F) detail of segment Ab 3, dorsal; (G) lateral seta with fine apex, adjacent to spiracle on abdominal segment Ab 4, dorsal; (H) lateral seta of Ab 7 with clavate apex, dorsal; (I) detail of tergum of Ab 3, lateral; (J–L) last abdominal segments, lateral, dorsal and ventral. Scale bars: 200 (A), 80 (B), 100 (C, D, G, K, L), 400 (E), 150 μm (F, H, I, J).


Fig. 7. Natural history of *P. hemera*: (A) Host plant, *Daphnopsis fasciculata* at the type locality; (B) seedling of *D. fasciculata* with several mines; (C) leaf with a single *P. hemera* mine on adaxial surface (closed and open arrows indicate the beginning and final portions of the mine); (D) sap-feeding larva, latero-dorsal view; (E) spinning larva, latero-dorsal; (F) pupal cocoon, dorsal; (G) pupa, dorsal; (H) pupal exuvium protruded from cocoon after adult emergence. Scale bars: 40 (B), 3 (C), 1 (D, E, G, H), 0.3 mm (F).

and filiform, reaching the last abdominal segments (Fig. 3C); proboscis extending to anterior margin of Ab 2; anterior, median and posterior legs reaching Ab 3, Ab 4 and Ab 7, respectively; forewings extending to the posterior portion of Ab 5 (Figs. 3C and 6E). A set of small, posteriorly directed spines, dorsally at the center from second to seventh abdominal segments (Fig. 6I); on tergum of the
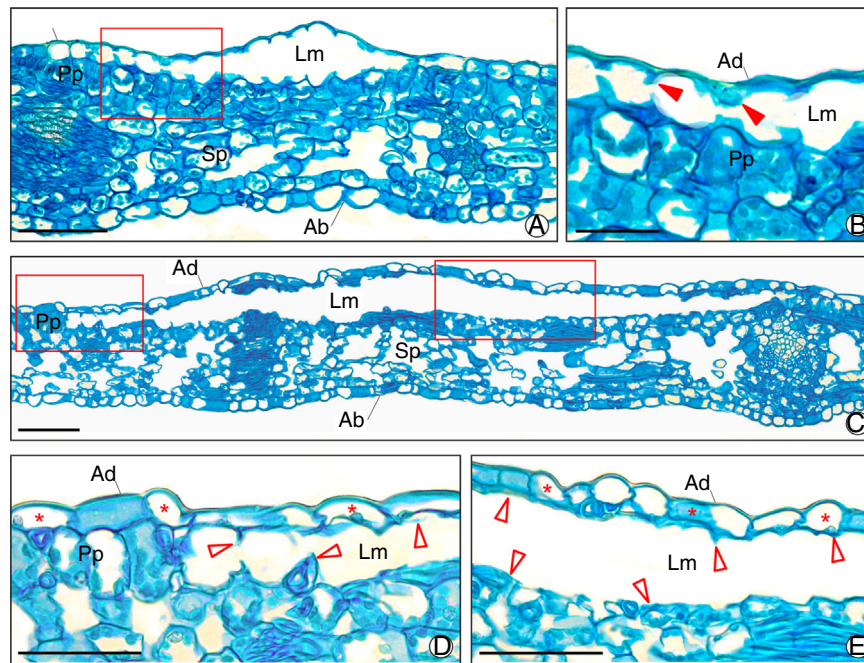
Fig. 8. Transverse histological sections of *P. hemera* mine on *Daphnopsis fasciculata* leaf. (A) initial portion (location indicated by dashed line in Fig. 7C); (B) detail of initial portion (enlarged area marked with a rectangle in A); (C) intermediate portion (location indicated by unbroken line in Fig. 7C); (D, E) details of intermediate portion (enlarged areas marked with rectangles in C). Asterisks indicate intact cells of epidermis. Closed and open arrows indicate cellular fragments left on epidermis and palisade parenchyma after feeding. Ab, abaxial surface of epidermis; Ad, adaxial surface of epidermis; Lm, leaf mine; Pp, palisade parenchyma; Sp, spongy parenchyma. Scale bars = 100 (A, C), 50 μm (B, D, E).
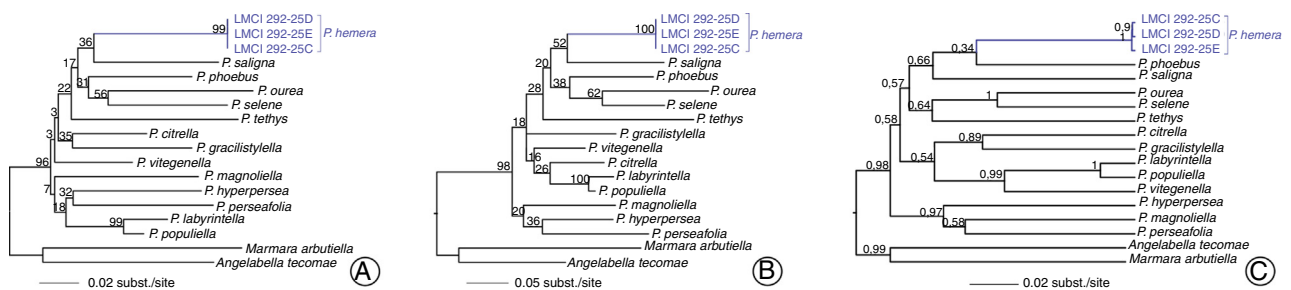
Fig. 9. Phylogenetic reconstruction for *P. hemera* based on 660 bp of the mitochondrial cytochrome oxidase c subunit I gene ('DNA barcode' region) using three methods: (A) distance (Neighbor-joining), (B) Maximum likelihood, and (C) Bayesian inference. Numbers above branches indicate node support (bootstrap for A and B and posterior probability for C). Samples in blue highlight the new taxon.

same abdominal segments, also one pair of stout spines and one pair of posteriorly directed small setae (Fig. 6E, F and I). A pair of medium-sized setae laterally on meso- and metathorax. One pair of setae with fine apex on pleura from Ab 2-5 (Fig. 6G); from Ab 6–7 the setae have clavate apex (Fig. 6H). Open spiracles present on Ab 2–7 (Fig. 6G). The eighth abdominal segment presents one pair of microsetae dorsolaterally on tergum, one pair of spiracles partially closed and one pair of medium-sized setae posteriorly directed (Fig. 6J and K). One pair of posteriorly directed, digitiform caudal processes on last abdominal segment (Fig. 6J–L).

Etymology. Hemera, in Greek mythology is the daughter of the night and represents the divinity that personifies the daylight, here making an allusion to the light and bright color of the forewings of this species.

Distribution. *P. hemera* is known only from its type locality, the Dense Umbrophilous Forest (= Atlantic Forest sensu stricto), CPCN Pró-Mata, São Francisco de Paula municipality, Rio Grande do Sul, Brazil.

Host plant (Fig. 7A). *D. fasciculata* (Meisn) Neveling (Thymelaeaceae). The host plant of *P. hemera* occurs as either a shrub or a small tree, endemic to Brazil and occurring in the following regions: Midwest (Distrito Federal), Southeast (Espírito Santo, Minas Gerais, Rio de Janeiro and São Paulo) and South (Paraná, Santa Catarina and Rio Grande do Sul) (Rossi, 2017).

Life history (Fig. 7B–H). Eggs of *P. hemera* are deposited on the adaxial leaf surface. After eclosion, the sap-feeding larva (Fig. 7D) penetrates the leaf blade starting the mine construction. In the beginning the mine is narrow and serpentine-shaped, increasing in width during development (Fig. 7B). Centrally along the mine a path of black feces left by the larva can be seen by transparency (Fig. 7B). Mines are initially constructed within the adaxial epidermal cells (Fig. 8A) by cutting the anticlinal cell walls (Fig. 8B). Later the larva goes deeper into leaf tissues and install within palisade parenchyma cells, also by cutting the anticlinal cell walls (Fig. 8C). The epidermal cells remain intact over the intermediary mine (Fig. 8C–E), while fragments of the anticlinal cell walls of the palisade parenchyma cells remain in the lateral portions of the mine (Fig. 8D) but are totally consumed in the central portion (Fig. 8E).

The spinning larva (Fig. 7E) does not feed and is responsible for the construction of the cocoon. This is endophylous and constructed at the final portion of the mine, and completely covered by whitish silk that provokes a slight leaf wrinkling (Fig. 7F). The pupal cocoon

is ruptured by the pupa's cocoon-cutter (Fig. 7G) during adult emergence. Later, the pupal exuvia is seen partially protruding from the cocoon (Fig. 7H). More than one mine were found in most of the mined leaves. A few mines were found on full grown *D. fasciculata* trees. The greatest density of leaves mined by *P. hemera* was found on young plants, especially those located in humid sections of trail borders existing in the type locality. The larvae were found active in the field from February to August, suggesting the species is multivoltine.

Phylogenetic inference

A total of 660 nucleotide sites were analyzed, of which 268 (40%) were variable. In accordance with our phylogenetic hypothesis, the monophyly of the new species was recovered in both methods of inference (distance and model-based), with high node support values (Fig. 9). Since the topologies were slightly different, all are presented. The sister relationship of *P. hemera* was not well resolved: node supports were quite low in all trees (NJ, Bayesian and ML). In the NJ and ML inferences, *P. hemera* clustered with *P. saligna* (Fig. 9). In the Bayesian analysis, the closest related lineage was *P. phoebus*; however, the node support (BPP) was very low. The genetic distance estimated between *P. hemera* and other taxa ranged from 14% to 20% (±2%) (see Supplementary Material; Fig. S1). The distance of the new species to the outgroups was 24% (±3%).

Discussion

P. hemera is described here based on morphological and molecular characters, showing enough stable characters in both types of analysis to separate it clearly from other congeneric species. Phylogeny showed a monophyletic status for the new species, but did not resolve close relationships. Different methods of reconstruction retrieved different results for sister taxa of *P. hemera*, although with low support. In the NJ and ML trees it was close to *P. salignela*, whereas in Bayesian inference it clustered with *P. phoebus*, a sympatric species from the same region of Atlantic Forest (Brito et al., 2017a). A comparative assessment of genetic distance to other Neotropical *Phyllocnistis* indicates a minimum of 12% for *P. hemera* to *P. citrella* and *P. vitegenella*, which indicates a great amount of divergence sampled in *Phyllocnistis*. Such high diversity is likely reflected in the evolutionary history reconstructed for the genera, e.g. by the absence of unknown lineages in the phylogeny, suggested by the putative long-branch attraction apparently found in *P. hemera* and *P. salignela* relationship (NJ and ML trees).

The forewing pattern of *P. hemera* resembles those described for congeneric species in the Neotropical region (Brito et al., 2017a), regarding number of fasciae and strigulae, presenting one well-marked longitudinal fascia, two visible transversal fasciae, three costal and four apical strigulae, the last emerging from the apical spot. Comparing *P. hemera* to the other congeneric Neotropical species the greatest similarity is found with *P. bourquini* Pastrana, a species described for Argentina; both species share forewing light yellow fasciae, but they can be contrasted by the morphology of the third and fourth fasciae, which are separated in *P. bourquini* and united in *P. hemera*. Another character that differentiates *P. hemera* from *P. drimiphaga* is the male valva; in *P. drimiphaga* the valva is divided into two lobes (Kawahara et al., 2009), the dorsal being more prominent than the ventral, while *P. hemera* has the distal portion of the valva undivided.

As already mentioned, the presence of ambulatory calli on the ventral region of meso- and metathorax in the spinning larva has already been described for *P. ourea*, also a species from the Atlantic forest. Ambulatory calli are not exclusive characters of Phyllocnistinae, and they also occur in representatives of the Oecophyllembiinae – *Angelabella* Vargas & Parra, *Eumetriochroa* Kumata, *Metriochroa* Busck and *Prophyllocnistis* Davis, a gracillariid subfamily closely related to the Phyllocnistinae (Vargas and Parra, 2005; Kumata, 1998; Busck, 1900; Davis, 1994; Kawahara et al., 2017). Stemmata have already been described for the sap-feeding larvae of some *Phyllocnistis* species of the Neotropical region, such as *P. ourea* Brito & Moreira and *P. selene* Brito & Moreira, which have two stemmata on the lateral region of the head. Thus *P. hemera* is the only species known so far with a single stemma followed by a microseta (Brito et al., 2017b).

The species described here is the first gracillariid associated with a Thymelaeaceae plant. As already described, *D. fasciculata* has a broad distribution in southeast Brazil (Rossi, 2017), suggesting that *P. hemera* might be distributed in other regions not evaluated in this study, which should be further explored. Interestingly, results presented here regarding the histology of the mine give further support for the existence of a broad feeding habit in relation to use of leaf tissues within *Phyllocnistis*. In other words, our data suggest that although highly species-specific to a given type of leaf tissue, species within this genus may use any kind of tissue, including the epidermis (e.g. *P. citrella*, Archor et al., 1997), spongy parenchyma (e.g. *P. tethys*, Brito et al., 2012), and palisade parenchyma (e.g. latter instars of *P. hemera*, as demonstrated here). The ultimate factors that lead to this variation in tissue usage remain to be determined. *P. hemera* uses the epidermis initially, and moves to the palisade parenchyma in the intermediary phase of the mine, which may indicate a search for better nutritional resources. Epidermal cells may function as lenses for capturing sunlight and as a consequence have large water-filled vacuoles and scarce cytoplasm. Palisade parenchyma cells, on the other hand, are commonly cytoplasm-rich, and may accumulate energetic molecules (Evert, 2006; Bowes and Mauseth, 2008).

The Atlantic forest is known for its extreme diversity with approximately 50% of the species considered endemics (Stemann et al., 2009). However, only five species of *Phyllocnistis* are known for the region (Brito et al., 2012, 2017a). As suggested by Brito et al. (2016), the vast majority of Neotropical gracillariid species remain to be discovered. Data presented in this study regarding a new species of *Phyllocnistis* for the Atlantic forest support further the hypothesis proposed by such authors in the sense that the scarcity of species described for the region in largely due to a lack of sampling, associated with a taxonomic impediment.

Conflicts of interest

The authors declare no conflicts of interest.

Appendix A. Supplementary data

Supplementary data associated with this article can be found, in the online version, at doi:10.1016/j.rbe.2017.11.001.

References

Achor, D.S., Browning, H., Albrigo, L.G., 1997. Anatomical and histochemical effects of feeding by Citrus leaf miner larvae (Phyllocnistis citrella Stainton) in Citrus leaves. J. Am. Soc. Horticult. Sci. 122, 829–836.

Bowes, B.G., Mauseth, J.D., 2008. Plant Structure: A Colour Guide, 2nd ed. Manson Publ Ltda, London.

Brito, R., Gonçalves, G.L., Vargas, H.A., Moreira, G.R.P., 2012. A new species of Phyllocnistis Zeller (Lepidoptera: Gracillariidae) from southern Brazil, with life-history description and genetic comparison to congeneric species. Zootaxa 3582, 1–16.

Brito, R., De Prins, J., De Prins, W., Mielke, O.H.H., Gonçalves, G.L., Moreira, G.R.P., 2016. Extant diversity and estimated number of Gracillariidae (Lepidoptera) species yet to be discovered in the Neotropical region. Rev. Bras. Entomol. 60, 275–283.

Brito, R., Mielke, O.H.H., Gonçalves, G.L., Moreira, G.R.P., 2017a. Description of three new species of Phyllocnistis Zeller, 1848 (Lepidoptera: Gracillariidae) from the Atlantic Forest, south Brazil, with notes on natural history and phylogeny. Austr. Entomol., http://dx.doi.org/10.1111/aen.12298.

Brito, R., Lopez-Vaamonde, C., Gonçalves, G.L., Mielke, O.H.H., Moreira, G.R.P., 2017b. Taxonomic revision of the Neotropical Phyllocnistis Zeller, 1848 (Lepidoptera: Gracillariidae), with descriptions of seven new species and host plant associations. Zootaxa 4341, 301–352.

Bukatsch, F., 1972. Bermerkungen zur Doppelfärbung Astrablau-Safranin. Mikrokosmos 61, 255.

Busck, A., 1900. New species of moths of the superfamily Tineina from Florida. Proc. United States Natl. Museum 23, 225–254.

Davis, D.R., 1987. Gracillariidae. In: Stehr, F.W. (Ed.), Immature Insects, vol. I. Kendall/Hunt Publishing Company, Dubuque, pp. 372–374.

Davis, D.R., 1994. Neotropical Microlepidoptera XXV. New leaf-mining moths from Chile, with remarks on the history and composition of Phyllocnistinae (Lepidoptera: Gracillariidae). Trop. Lepidoptera 5, 65–75.

Davis, D.R., Wagner, D.L., 2011. Biology and systematics of the New World Phyllocnistis Zeller leafminers of the avocado genus Persea (Lepidoptera, Gracillariidae). ZooKeys 97, 39–73.

De Prins, J., Brito, R., Moreira, G.R.P., 2016. An annotated taxonomic checklist of the Neotropical Gracillariidae (Lepidoptera) with links to the information on host plants and parasitoids. Zootaxa 4158, 1–51.

De Prins, J., De Prins, W., 2017. Global Taxonomic Database of Gracillariidae (Lepidoptera), http://www.gracillariidae.net (accessed August 2017).

Drummond, A.J., Rambaut, A., 2007. BEAST: Bayesian evolutionary analysis by sampling trees. BMC Evol. Biol. 7, 214.

Drummond, A.J., Suchard, M.A., Xie, D., Rambaut, A., 2012. Bayesian phylogenetics with BEAUti and the BEAST 1.7. Mol. Biol. Evol. 29, 1969–1973.

Evert, R.F., 2006. Esau's Plant Anatomy, 3rd ed. John, Wiley & Sons, Inc., New Jersey.

Felsenstein, J., 1985. Confidence limits on phylogenies: an approach using the bootstrap. Evolution 39, 783–791.

Folmer, O., Black, M., Hoeh, W., Lutz, R., Vrijenhoek, R., 1994. DNA primers for amplification of mitochondrial cytochrome c oxidase subunit I from diverse metazoan invertebrates. Mol. Mar. Biol. Biotechnol. 3, 294–299.

Hebert, P.D.N., Cywinska, A., Ball, S.L., deWaard, J.R., 2003. Biological identifications through DNA barcodes. Proc. R. Soc. B Biol. Sci. 270, 313–321.

Kawahara, A.Y., Nishida, K., Davis, D.R., 2009. Systematics, host plants, and life histories of three new Phyllocnistis species from the central highlands of Costa Rica (Lepidoptera, Gracillariidae, Phyllocnistinae). ZooKeys 27, 7–30.

Kawahara, A.Y., Plotkin, D., Ohshima, I., Lopez-Vaamonde, C., Houlihan, P., Breinholt, J.W., Kawakita, A., Xiao, L., Regier, J.C., Davis, D.R., Kumata, T., Sohn, J.C., De Prins, J., Mitter, C., 2017. A molecular phylogeny and revised higher-level classification for the leaf-mining moth family Gracillariidae and its implications for larval host use evolution. Syst. Entomol. 42, 60–81.

Kobayashi, S., Hirowatari, T., 2011. Two Chloranthaceae leafminers of the genus Phyllocnistis (Lepidoptera: Gracillariidae: Phyllocnistinae) from Japan, with descriptions of new species and pupal morphology. Lepidoptera Sci. 62, 156–165.

Kumata, T., 1998. Japanese species of the subfamily Oecophyllembiinae Réal and Balachowsky (Lepidoptera: Gracillariidae), with descriptions of a new genus and eight new species. Insecta Matsumurana 54, 77–131.

Paiva, J.G.A., Fank-De-Carvalho, S.M., Magalhães, M.P., Graciano-Ribeiro, D., 2006. Verniz vitral incolor 500® : uma alternativa de meio de montagem economicamente viável. Acta Bot. Bras. 20, 257–264.

Rossi, L., 2017. Thymelaeaceae in Flora do Brasil 2020 em construção. Jardim Botânico do Rio de Janeiro, http://floradobrasil.jbrj.gov.br/reflora/floradobrasil/FB14944 (accessed August 2017).

Stemann, J.R., Forzza, R.C., Salino, A., Sobral, M., Costa, D.P., Kamino, L.H.Y. (Eds.), 2009. Plantas da Floresta Atlântica. Instituto de Pesquisas Jardim Botânico do Rio de Janeiro, Rio de Janeiro, 509 pp.

Tamura, K., Peterson, D., Peterson, N., Stecher, G., Nei, M., Kumar, S., 2011. MEGA5: molecular evolutionary genetics analysis using maximum likelihood, evolutionary distance and maximum parsimony methods. Mol. Biol. Evol. 28, 2731–2739.

Vargas, H.A., Parra, L.E., 2005. Um nuevo género y una nueva especie de Oecophyllembiinae (Lepidoptera: Gracillariidae) de Chile. Neotrop. Entomol. 34, 227–233.